The N terminus of Orai1 couples to the AKAP79 signaling complex to drive NFAT1 activation by local Ca^{2+} entry

Pulak Kar[a], Yu-Ping Lin[a,b], Rajesh Bhardwaj[c], Charles J. Tucker[b], Gary S. Bird[b], Matthias A. Hediger[c], Carina Monico[d], Nader Amin[e], and Anant B. Parekh[a,b,1]

[a]Department of Physiology, Anatomy and Genetics, Oxford University, Oxford OX1 3PT, United Kingdom; [b]Laboratory of Signal Transduction, National Institute of Environmental Health Sciences, NIH, Research Triangle Park, NC 27709; [c]Department of Nephrology and Hypertension, University Hospital Bern, Inselspital, 3010 Bern, Switzerland; [d]Micron Oxford Advanced Bioimaging Unit, Department of Biochemistry, Oxford University, Oxford OX1 3QU, United Kingdom; and [e]Department of Chemistry, Oxford University, Oxford OX1 3TA, United Kingdom

Edited by Michael D. Cahalan, University of California, Irvine, CA, and approved March 10, 2021 (received for review June 22, 2020)

To avoid conflicting and deleterious outcomes, eukaryotic cells often confine second messengers to spatially restricted subcompartments. The smallest signaling unit is the Ca^{2+} nanodomain, which forms when Ca^{2+} channels open. Ca^{2+} nanodomains arising from store-operated Orai1 Ca^{2+} channels stimulate the protein phosphatase calcineurin to activate the transcription factor nuclear factor of activated T cells (NFAT). Here, we show that NFAT1 tethered directly to the scaffolding protein AKAP79 (A-kinase anchoring protein 79) is activated by local Ca^{2+} entry, providing a mechanism to selectively recruit a transcription factor. We identify the region on the N terminus of Orai1 that interacts with AKAP79 and demonstrate that this site is essential for physiological excitation–transcription coupling. NMR structural analysis of the AKAP binding domain reveals a compact shape with several proline-driven turns. Orai2 and Orai3, isoforms of Orai1, lack this region and therefore are less able to engage AKAP79 and activate NFAT. A shorter, naturally occurring Orai1 protein that arises from alternative translation initiation also lacks the AKAP79-interaction site and fails to activate NFAT1. Interfering with Orai1–AKAP79 interaction suppresses cytokine production, leaving other Ca^{2+} channel functions intact. Our results reveal the mechanistic basis for how a subtype of a widely expressed Ca^{2+} channel is able to activate a vital transcription pathway and identify an approach for generation of immunosuppressant drugs.

calcium channel | transcription factor | store-operated | AKAP79

Innate and adaptive immunity require stimulus-dependent nuclear transcription, a form of signaling that is contingent upon a dialogue between the plasma membrane and nucleus. Events at the cell surface are conveyed to the nucleus through recruitment of transcription factors such as members of the nuclear factor of activated T cells (NFAT), which are important for growth, development and function of the immune, cardiovascular and nervous systems (1). Four members of the NFAT family (NFAT1–4) are held in an inactive state at rest by extensive phosphorylation of multiple serine and threonine residues (2). Dephosphorylation by the Ca^{2+}-activated protein phosphatase calcineurin, the target for immunosuppressants, exposes a nuclear localization sequence enabling these NFAT isoforms to migrate into the nucleus to regulate transcriptional activity of various chemokine and cytokine genes (3).

The demonstration that a loss-of-function mutation in the store-operated Ca^{2+} channel Orai1 prevented NFAT activation in T cells and led to a devastating severe combined immunodeficiency (4) focused attention on the specific line of communication between Orai1 and NFAT. We have demonstrated that Ca^{2+} nanodomains generated by open Orai1 channels, which extend just a few nanometers below the plasma membrane, activate NFAT1 and NFAT4 isoforms (5, 6). Calcineurin is not associated with Orai1 channels directly but is brought into the realm of the Ca^{2+} nanodomain by the scaffolding protein AKAP79 (A-kinase anchoring protein 79) (7). AKAP79 binds both calcineurin and NFAT and therefore positions the enzyme close to its target. In nonstimulated cells, AKAP79 weakly associates with Orai1 but, after stimulation, it interacts with the Ca^{2+} channel to form a membrane-delimited signaling complex in which calcineurin is activated by local Ca^{2+} to dephosphorylate and release NFAT1 (7). Our previous work showed that Orai3, unlike Orai1, was unable to activate NFAT (7). The difference between their respective abilities to interact with AKAP79 resided within the N terminus of the channels; the N terminus of Orai1 was essential for coupling to the AKAP79-NFAT pathway (7). However, the structural requirements within the N terminus of Orai1 for interaction with AKAP79 remain elusive.

In addition to Orai1, two other paralogues are expressed in mammalian cells, Orai2 and Orai3 (8). Further complexity is increased by the discovery that alternative translation initiation of Orai1 gives rise to long (Orai1α) and short (Oraiβ) forms, differing in the lengths of their respective N termini (9). Whether both Orai1 forms interact with AKAP79 and thereby activate NFAT1 is unknown.

In this study, we identify the region on the N terminus of Orai1 that is important for interaction with AKAP79 and exploit this to demonstrate that NFAT1 activation to physiological levels of receptor stimulation is wholly dependent on interaction of AKAP79 and Orai1 at native levels of expression. Interfering

Significance

Store-operated Orai1 Ca^{2+} channels are a major route for trigger Ca^{2+} in immune cells. Local Ca^{2+} entry through the channels activates NFAT transcription factors, which in turn increase expression of chemokines and cytokines that orchestrate inflammatory responses. We identify a region on the N terminus of Orai1 that is indispensable for activating NFAT, through interaction with the scaffolding protein AKAP79. We show that a peptide that uncouples Orai1 from AKAP79 suppresses cytokine production, leaving other functional consequences of the channel intact. Our results identify an approach for developing immunosuppressant drugs.

Author contributions: P.K., Y.-P.L., and A.B.P. designed research; P.K., Y.-P.L., R.B., C.J.T., G.S.B., C.M., and N.A. performed research; R.B. and M.A.H. contributed new reagents/analytic tools; P.K., Y.-P.L., C.J.T., G.S.B., C.M., N.A., and A.B.P. analyzed data; and A.B.P. wrote the paper.

The authors declare no competing interest.

This article is a PNAS Direct Submission.

[1]To whom correspondence may be addressed. Email: anant.parekh@nih.gov.

This article contains supporting information online at https://www.pnas.org/lookup/suppl/doi:10.1073/pnas.2012908118/-/DCSupplemental.

Published May 3, 2021.

with the AKAP79 interaction site on Orai1 fails to affect other Ca^{2+}-dependent responses such as exocytosis. Finally, we show that the Orai1 region that interacts with AKAP79 is present in Orai1α but not Orai1β and is absent in other Orai paralogues, providing a molecular basis for selective recruitment of Ca^{2+}-sensitive responses by Orai1 channels.

Results

AKAP79 Is Essential for Physiological Activation of NFAT1 but Not for Cytosolic Ca^{2+} Oscillations. Knockdown of AKAP79 suppresses activation of NFAT1 by CRAC channels following stimulation with thapsigargin, a pharmacological tool that depletes intracellular Ca^{2+} stores by inhibition of the SERCA pump (7). To see whether AKAP79 played an indispensable role under physiological conditions, we measured NFAT1 migration into the nucleus following stimulation of Gq-coupled cysteinyl leukotriene type I receptors with the agonist leukotriene C_4 (LTC_4). Exposure to low concentrations of LTC_4 elicits a series of repetitive cytosolic Ca^{2+} oscillations in RBL cells (10), thought to be the physiologically relevant form of intracellular Ca^{2+} signaling. These oscillations arise from regenerative Ca^{2+} release from $InsP_3$-sensitive Ca^{2+} stores followed by Ca^{2+} entry through CRAC channels, which replete the stores with Ca^{2+} in readiness for the next oscillatory cycle (10). The number and peak amplitude of the oscillations run down gradually over time, due to receptor desensitization (11). Cytosolic Ca^{2+} oscillations to LTC_4 are inhibited, and to similar extents, by removal of external Ca^{2+}, after knockdown of Orai1 or after pharmacological block of the channels (12). Local Ca^{2+} entry through CRAC channels and not the oscillatory bulk cytosolic Ca^{2+} rise activates NFAT1 (13). We repeated these experiments but now in HEK293 cells due to their ease of transfection, the need to express various Orai1 and AKAP79 mutants together, and because some experiments below required the use of an Orai knockout cell line. Initial experiments failed to reliably observe cytosolic Ca^{2+} oscillations to reported endogenous agonists including acetylcholine in our HEK293 cell line. We therefore expressed the cysteinyl leukotriene type 1 receptor in these cells. Stimulation with 160 nM LTC_4 evoked oscillations in cytosolic Ca^{2+} that gradually ran down with time (Fig. 1 *A–D*). Loss of the oscillatory Ca^{2+} signals occurred rapidly after inhibition of CRAC channels with BTP2 (*SI Appendix*, Fig. S1). Stimulation with LTC_4 led to robust nuclear accumulation of NFAT1-GFP, which was inhibited by BTP2 (Fig. 1 *E* and *F*). Small interfering RNA (siRNA)-targeted knockdown of AKAP79 results in ∼75% reduction in protein levels (7) (Fig. 1 *G* and *H*). Cytosolic Ca^{2+} oscillations to LTC_4 were unaffected by the loss of AKAP79 (Fig. 1 *B–D*) but NFAT1 translocation was almost suppressed (Fig. 1 *E* and *F*). Expression of calcineurin was not affected by knockdown of AKAP79 (Fig. 1 *G* and *H*). Furthermore, nuclear accumulation of NFAT1-GFP in AKAP79-deficient cells stimulated with LTC_4 could be rescued by application of a high dose of the Ca^{2+} ionophore ionomycin (Fig. 1*F*), which induces a large rise in bulk cytosolic Ca^{2+} independently of CRAC channels (10). Therefore, the inability of leukotriene receptors to activate NFAT1 in the absence of AKAP79 is not due to loss of cytosolic Ca^{2+} signaling, to altered expression of calcineurin, or to suppression of the NFAT pathway per se.

Ca^{2+}-dependent production of adenosine 3′,5′-cyclic monophosphate (cAMP) followed by stimulation of protein kinase A tethered to AKAP79 has been reported to phosphorylate serine 34 on Orai1, causing Ca^{2+}-dependent inactivation (CDI) of channels and leading to slightly faster rundown of Ca^{2+} oscillations evoked by muscarinic receptor stimulation (14). One would therefore have expected knockdown of AKAP79 to reduce the ability of tethered protein kinase from phosphorylating Orai1, changing oscillation frequency. We observed no change over a 10-min recording period (Fig. 1 *B–D*). It is possible that effects might have been revealed over a much longer time frame, particularly as the protein kinase A-driven change in Ca^{2+} oscillation frequency was modest, decreasing the number of oscillations by one over 15-min recording (14).

CRAC Channels Selectively Activate NFAT that Is Tethered to AKAP79. A fraction of the total cellular pool of NFAT is bound to AKAP79 (7, 15). Recently, a leucine zipper domain on the C terminus of AKAP79 was reported to bind NFAT4 (16). To test whether NFAT bound to AKAP79 was activated by Ca^{2+} entry through CRAC channels, we knocked down endogenous AKAP79 and then expressed either wild-type protein or protein in which the leucine zipper region had been deleted (AKAP79ΔLZ), both tagged with YFP. Pull-down experiments demonstrated that NFAT1 binding to AKAP79 was significantly reduced by deletion of the leucine zipper domain (*SI Appendix*, Fig. S2), and to an extent similar to that reported for NFAT4 (16). Because knockdown of AKAP79 results in typically 70 to 80% reduction in protein levels (7) (Fig. 1 *G* and *H*) and AKAP79 forms dimers (17), the remaining endogenous AKAP79 could contribute to the extent of NFAT pulldown by AKAP79-YFP. Therefore, the real difference in NFAT association between AKAP79 and AKAPΔLZ is likely larger than observed but is obscured by the background in the assay. However, we cannot rule out the possibility of a second NFAT-binding site on AKAP79 distinct from that in the leucine zipper region.

Surface expression of AKAP79ΔLZ was similar to that of wild-type protein (Fig. 1*I*). Whereas robust movement of NFAT1 into the nucleus occurred when CRAC channels opened in the presence of wild-type AKAP79, NFAT nuclear migration was reduced when AKAP79ΔLZ was expressed instead (Fig. 1 *J* and *K*). AKAP79ΔLZ associated with Orai1 after store depletion and to an extent that was indistinguishable from that of wild-type Orai1 (*SI Appendix*, Fig. S3). AKAP79ΔLZ-expressing cells retained the ability to activate NFAT1 in a Ca^{2+}-dependent manner because stimulation with a high dose of ionomycin rescued NFAT1 migration into the nucleus (Fig. 1*K*). These findings reinforce the central role of local communication between CRAC channels and AKAP79 for effective activation of NFAT1.

Proximity Ligation Assay Reveals Increased Colocalization between Orai1 and AKAP79 after Stimulation. Pull-down studies have shown that AKAP79 and Orai1 interact after store depletion (7). We used a proximity ligation assay to visualize Orai1-AKAP79 colocalization before and after stimulation. In this assay, proximity of two proteins is reflected in the presence of discrete spots. Cells were cotransfected with AKAP79-YFP, Orai1-myc, and untagged STIM1. In resting cells, some overlap of AKAP79 and Orai1 was observed (Fig. 2 *A* and *B*), consistent with a report of a modest fluorescence resonance energy transfer signal between the two proteins under unstimulated conditions (14). After stimulation with thapsigargin, however, significantly more spots were observed (Fig. 2 *A* and *B*), reflecting increased colocalization between AKAP79 and Orai1. We repeated these experiments but expressed AKAP79ΔLZ instead. Some colocalization was observed under resting conditions, and this increased significantly after stimulation (Fig. 2 *A* and *B*). These findings are in good agreement with the earlier pull-down study (7) and further show that AKAP79ΔLZ interacts with Orai1 in a manner similar to that of AKAP79, consistent with the pull-down experiments in *SI Appendix*, Fig. S3.

Orai1α but Not Orai1β Activates NFAT1. Our previous chimeric studies demonstrated that the N terminus of Orai1 was important for coupling to AKAP79 (7). However, the region on the N terminus that interacts with AKAP79 is unknown. Orai1β translation is initiated from a second initiator methionine that is 63 amino acids downstream from the first initiation site for Orai1α and therefore has a considerably shorter N terminus (9). We mapped the AKAP79 association region by comparing the relative abilities of Orai1α and Orai1β to activate NFAT1. To prevent a

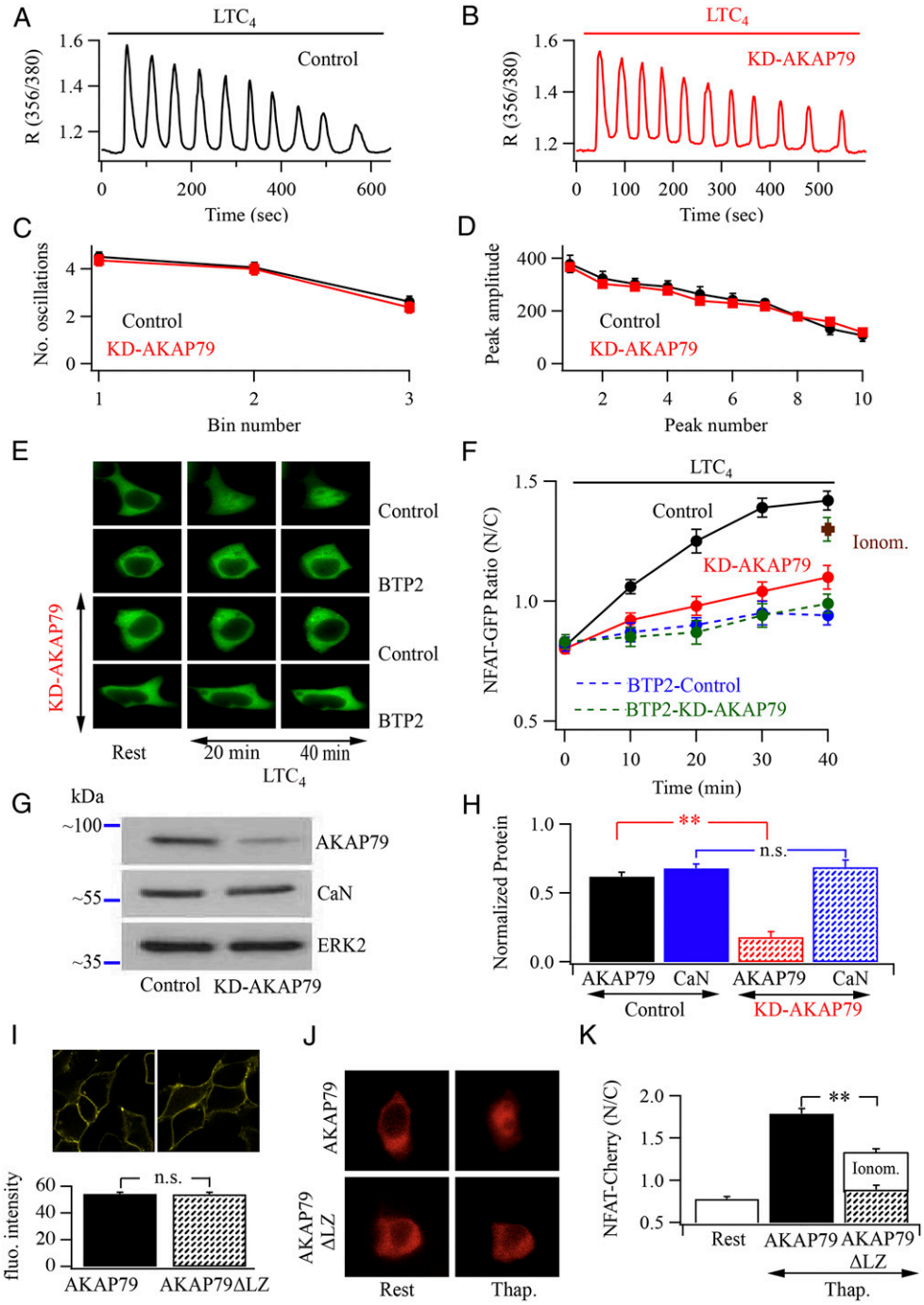

Fig. 1. AKAP79 knockdown suppresses NFAT1 translocation but does not affect cytosolic Ca^{2+} oscillations. (*A*) Stimulation with 160 nM LTC_4 evokes repetitive Ca^{2+} oscillations in 2 mM external Ca^{2+} solution. (*B*) Cytosolic Ca^{2+} oscillations to LTC_4 are maintained after knockdown of AKAP79 (denoted KD-AKAP79). (*C*) Aggregate data compare the number of oscillations from several experiments. Each point is the mean of between 17 and 20 cells. Data were binned in intervals of 200 s. (*D*) As in *C*, but the peak amplitude of each oscillation is compared. (*E*) Images compare nuclear accumulation of NFAT1-GFP in resting cells and then after stimulation with LTC_4 for the times indicated. Each row represents the same cell. BTP2 denotes cells pretreated for 10 min with the CRAC channel blocker (10 μM). (*F*) Time course of NFAT1-GFP translocation to the nucleus is compared for the conditions shown. Each point is the mean of >10 cells. The single point labeled Ionom. denotes rescue ($P < 0.01$) of NFAT1-GFP translocation in AKAP79-deficient cells when ionomycin (1 μM) was applied 40 min after LTC_4. (*G*) Western blot compares protein levels of AKAP79, calcineurin (CaN), and ERK2 (marker) in control cells and after knockdown of AKAP79. (*H*) Bar chart shows relative protein expression (normalized to ERK2) for the conditions shown. (*I*) Images show surface expression in cells expressing either wild-type AKAP79-YFP or AKAP79ΔLZ-YFP. In these experiments, endogenous AKAP79 was knocked down 24 h before transfection with either AKAP-YFP construct. Bar chart compares YFP intensity at the cell periphery for the two conditions. (*J*) Images compare NFAT1-mCherry nuclear translocation in cells expressing either AKAP79 or AKAP79ΔLZ at rest and then after thapsigargin stimulation. (*K*) Aggregate data from experiments as in *J* are show. Data are the mean of between eight and 12 cells. Ionomycin was applied for 20 min, 40 min after thapsigargin stimulation. The symbol ** compares responses between AKAP79 and AKAP79ΔLZ groups, the latter prior to ionomycin stimulation. In *F*, apart from $t = 0$, all points in control graph are significantly different from corresponding points on the three other graphs. The point at $t = 40$ min for control was not significantly different from the point labeled Ionom. ($P > 0.1$). In *C*, *D*, *F*, *H*, *I*, and *K*, all data are shown as mean± SEM. $^{**}P < 0.01$; n.s., not significant. All data were from HEK293 cells.

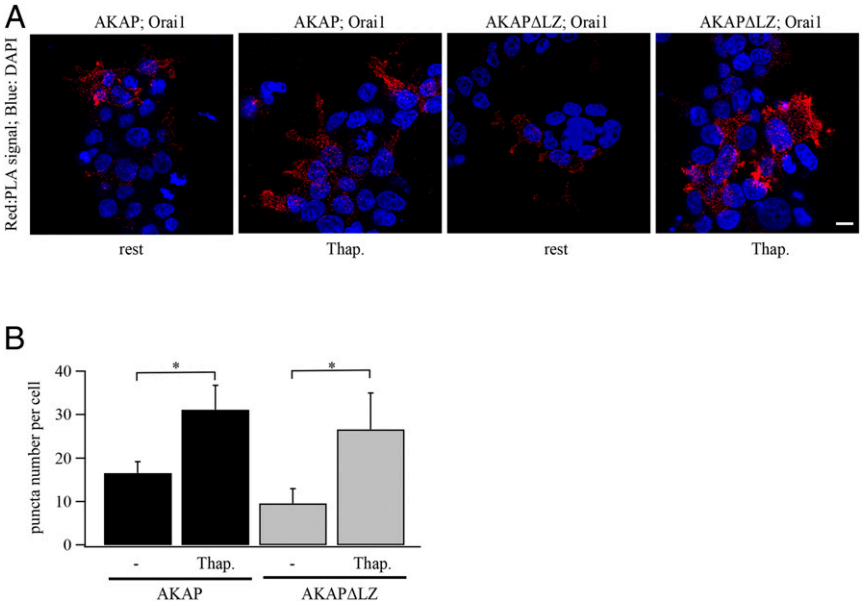

Fig. 2. Proximity ligation assay (PLA) shows increased association of AKAP79 with Orai1 after stimulation in HEK293 cells. (*A*) Images compare proximity of AKAP79-YFP and Orai1-myc in HEK293 cells at rest and then after 15-min exposure to thapsigargin. The two panels on the right show corresponding images for cells expressing AKAP79ΔLZ and Orai1-myc. (*B*) Aggregate data from two independent experiments are compared (>50 cells per bar). *$P < 0.05$. (Scale bar, 10 μm.)

contribution from endogenous Orai1 protein, we first knocked down the channels using an siRNA construct that targeted both Orai1α and Orai1β. Endogenous Orai1 protein was reduced by ~80% 24 h after siRNA transfection (7) and store-operated Ca^{2+} entry was reduced by >85% (*SI Appendix*, Fig. S4, labeled O1KD). We then expressed either Orai1α-GFP or Orai1β-GFP together with STIM1 and NFAT1-mCherry. Both Ca^{2+} release from thapsigargin-sensitive Ca^{2+} stores and store-operated Ca^{2+} entry was similar in cells expressing either Orai1α or Orai1β (Fig. 3*A*; aggregate data summarized in Fig. 3*B*). However, NFAT1-mCherry only migrated into the nucleus when Orai1α was expressed; no detectable movement was seen following activation of Orai1β (Fig. 3 *C* and *D*). To see whether this difference was a consequence of differential interaction with AKAP79, we immunoprecipitated either Orai1α-GFP or Orai1β-GFP and then immunoblotted for endogenous AKAP79. Robust association of Orai1α-GFP with AKAP79 was observed in thapsigargin-treated cells (Fig. 3*E*). By contrast, despite similar levels of protein expression, interaction between Orai1β-GFP and AKAP79 was relatively weak (Fig. 3*E*). These results demonstrate that a region within the first 63 amino acids in the N terminus of Orai1α is necessary for interaction with AKAP79. To confirm this, we expressed an Orai1 channel lacking the first 89 amino acids in the N terminus (ΔN-Orai1-YFP; labeled ΔN-O1). Although ΔN-Orai1-YFP was located at the cell surface (Fig. 3*C*), it failed to activate NFAT1 (Fig. 3 *C* and *D*), as loss of the N terminus leads to a loss of Orai1 channel activity (18). Importantly, ΔN-Orai1 failed to associate with AKAP79 after store depletion with thapsigargin (Fig. 3*F*).

We considered the possibility that the cytosolic Ca^{2+} signals differed between Orai1α and Orai1β over a time course of tens of minutes, and this explained the dramatic difference in NFAT movement. To address this, we measured cytosolic Ca^{2+} and NFAT1 translocation at the same time in an HEK293 cell line in which all Orai genes (Orai1, 2, and 3) had been knocked out using CRISPR-Cas9 gene editing (labeled TKO HEK for triple-knockout HEK; see *Materials and Methods* and *SI Appendix*). For indistinguishable cytosolic Ca^{2+} signals (*SI Appendix*, Fig. S5*A*), NFAT1 translocated to the nucleus only when Orai1α was expressed (*SI Appendix*, Fig. S5*B*). Averaged data from many cells showed that, despite evoking a similar cytosolic Ca^{2+} signal, Orai1β was unable to stimulate NFAT1 translocation to the nucleus (*SI Appendix*, Fig. S5 *C* and *D*).

A previous study reported that Orai1β was capable of activating NFAT, due to reduced CDI of the channels arising from the absence of serine 34, the target for protein kinase A (14). However, other studies have found that CDI is unaffected by deletion of regions of the N terminus that include S34 (19, 20). For similar bulk cytosolic Ca^{2+} signals, we find that Orai1α is considerably more effective than Orai1β in activating NFAT1 (*SI Appendix*, Fig. S5). It is possible that a much larger Ca^{2+} rise, due to cells expressing more Orai1β than Orai1α activates NFAT1, in a manner analogous to other agents that induce a large bulk rise in cytosolic Ca^{2+} (13).

Mapping the AKAP Association Region on Orai1. To identify regions in Orai1 that associate with AKAP79, we made various N-terminal deletion mutants and evaluated the impact of these constructs on store-operated Ca^{2+} entry, NFAT1 activation, and interaction with AKAP79. Responses were compared with cells overexpressing wild-type Orai1 to a similar extent. In these experiments, endogenous Orai1 protein was knocked down and STIM1 was coexpressed with the various Orai1 constructs. For cells expressing either wild-type Orai1-YFP or Orai1 lacking amino acids 2 to 14 in the N terminus [(V(2-14)N-Orai1-YFP)], store-operated Ca^{2+} entry was unaltered (Fig. 4 *A* and *B*). Migration of NFAT1-cherry into the nucleus was also similar between cells expressing wild-type Orai1-YFP and V(2-14)N-Orai1-YFP (Fig. 4 *C* and *D*). Following immunoprecipitation of Orai1-YFP or V(2-14)N-Orai1-YFP after thapsigargin stimulation, AKAP79 was detected in either immunoblot (Fig. 4*E*). Therefore, amino acid residues 2 to 14 in the N terminus of Orai1 do not contribute to AKAP association region (AKAR).

Similar results were obtained when amino acids 17 to 37 in the N terminus were removed instead [V(17-37)N-Orai1-YFP]. Following stimulation with thapsigargin, store-operated Ca^{2+} entry (Fig. 4 *A* and *B*), NFAT1-mCherry nuclear accumulation (Fig. 4 *C* and *D*) and association with AKAP79 (Fig. 4*E*) were all very similar to those seen with wild-type Orai1-YFP. By contrast, deletion of amino acids 39 to 59 in the N terminus of Orai1

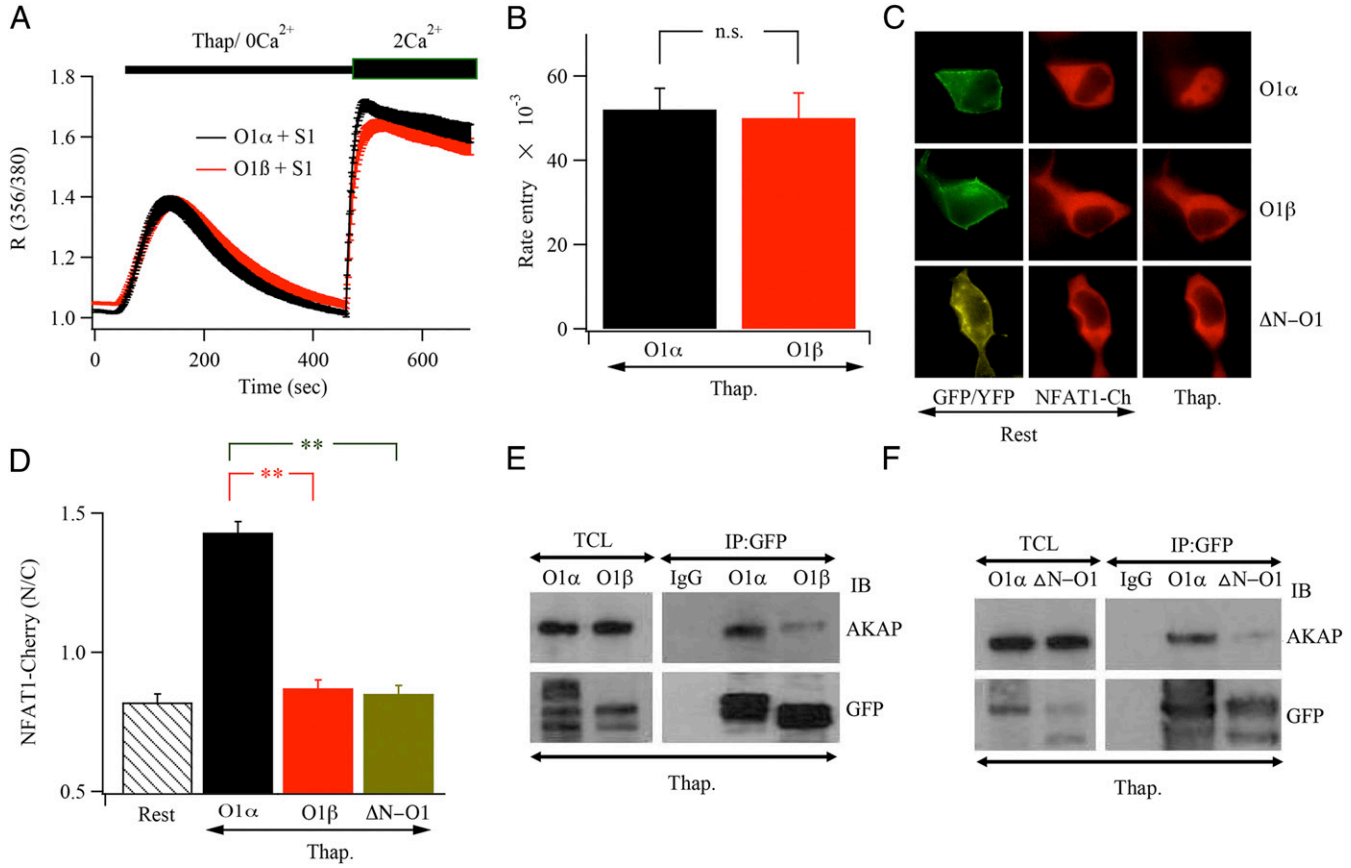

Fig. 3. Orai1α, but not Orai1β, interacts with AKAP79. (*A*) Traces compare Ca^{2+} release and subsequent store-operated Ca^{2+} entry evoked by thapsigargin in cells expressing either Orai1α or Orai1β. Each trace is the mean of at least 50 cells. (*B*) Bar chart compares rate of store-operated Ca^{2+} entry for the conditions shown, obtained as in *A*. (*C*) NFAT1-mCherry translocation is compared following expression of Orai1α-GFP, Orai1β-GFP, or Δ(1-89)-Orai1-YFP (labeled ΔN-O1) proteins. Rest denotes nonstimulated conditions. (*D*) Aggregate data from several experiments as in *C* are compared. Each bar denotes between 12 and 17 cells. (*E*) Orai1-GFP proteins were immunoprecipitated and then blotted for AKAP79. TCL denotes total cell lysate. (*F*) Orai1α interacts with AKAP79 after thapsigargin stimulation but ΔN-Orai1 does not. In all experiments shown, endogenous Orai1 was knocked down 24 h prior to transfection with Orai1α, Orai1β, or ΔN-Orai1 plasmid together with untagged STIM1. In *A*, *B*, and *D*, data are shown as mean± SEM. $^{**}P < 0.01$; n.s., not significant. All data were from HEK 293 cells.

[V(39-59)N-Orai1-YFP] suppressed NFAT1-mCherry migration to the nucleus following exposure to thapsigargin (Fig. 4 *C* and *D*). Importantly, AKAP79 no longer interacted with V(39-59) N-Orai1-YFP (Fig. 4*E*). Store-operated Ca^{2+} entry in cells expressing V(39-59)N-Orai1-YFP was similar to that seen in corresponding control cells (Fig. 4 *A* and *B*). In thapsigargin-treated cells expressing V(39-59)N-Orai1-YFP, NFAT1-mCherry migration to the nucleus could be rescued by application of a high concentration of ionomycin (Fig. 4 *C* and *D*), demonstrating the NFAT1 pathway was not suppressed itself by the presence of V(39-59)N-Orai1-YFP. Collectively, these deletion studies identify AKAR to include amino acids 39 and 59 in the N terminus of Orai1.

AKAP79 Interaction Is Specific to the Orai1 Paralogue. Sequence alignments show that AKAR is contained within the N terminus of Orai1 but not in the N terminus of Orai2 or Orai3 paralogues (*SI Appendix*, Fig. S6). A prediction would therefore be that neither Orai2 nor Orai3 couples to AKAP79 after store depletion and therefore does not activate NFAT1 following local Ca^{2+} entry through CRAC channels. To test this, we knocked down endogenous Orai1 and then transfected cells with Orai1-, Orai2-, or Orai3-YFP together with STIM1. Activation of store-operated Orai1 channels resulted in robust nuclear accumulation of NFAT1-cherry (Fig. 4 *F* and *G*). However, little nuclear migration of NFAT1-cherry occurred following opening of either store-operated Orai2 or Orai3 channels (Fig. 4 *F* and *G*). Nuclear migration could be triggered by the subsequent application of a high dose of ionomycin, confirming that the NFAT1 translocation pathway was indeed active in all these cells (Fig. 4 *F* and *G*). We confirmed these findings using the Orai TKO cell line. Stimulation with thapsigargin in the presence of external Ca^{2+} evoked only a transient rise in cytosolic Ca^{2+} in TKO cells, reflecting Ca^{2+} release from the stores, consistent with the absence of store-operated Ca^{2+} entry (Fig. 4*H*). Expression of each Orai paralogue with STIM1 led to a sustained cytosolic Ca^{2+} signal, measured over 40 min, with the profile of Orai1 > Orai2 > Orai3 (*SI Appendix*, Fig. S7), as reported recently using a different TKO HEK cell line (21). We noticed that the amplitude and time course of the Ca^{2+} signal in Orai3-expressing TKO cells was similar to that seen in wild-type HEK293 cells (where the dominant functional isoform is Orai1) overexpressing STIM1, measured over 40 min (Fig. 4*H* and *SI Appendix*, Fig. S7). However, activation of NFAT occurred only in wild-type cells; TKO cells expressing Orai3 were unable to stimulate NFAT (Fig. 4*I*), despite similar bulk cytosolic Ca^{2+} signals (Fig. 4*H*).

To confirm that the N terminus of Orai1 was critical for coupling to NFAT, we carried out a reversal of the chimeric experiment we had reported earlier (7). In that study, we made an Orai3 chimera, which comprised Orai3 but with the N terminus replaced by the N terminus of Orai1 (called N1-O3). Whereas Orai3 was unable to activate NFAT, the chimera was effective. To test the importance of the N terminus in a different way, we expressed an Orai1-YFP construct in which the N

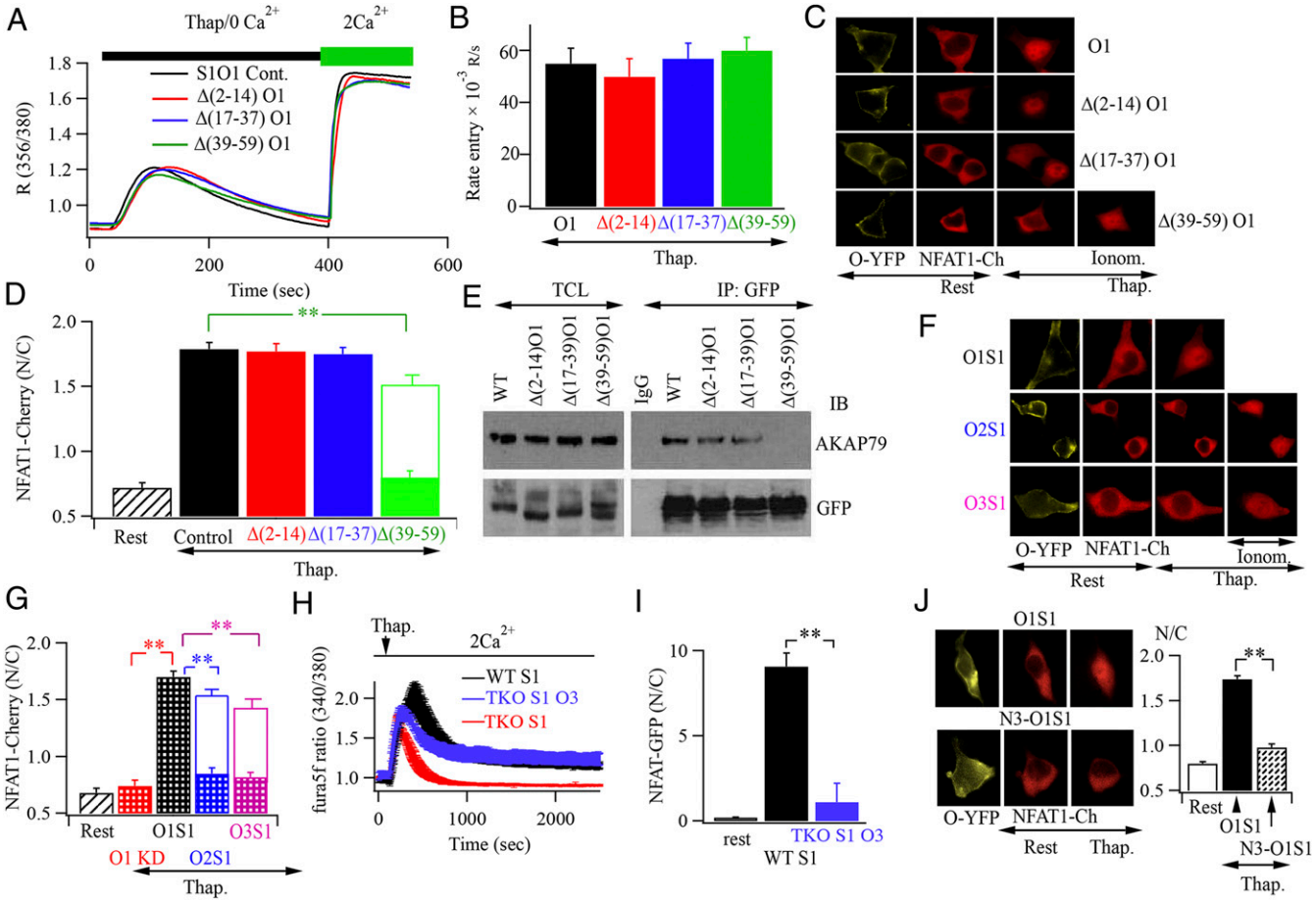

Fig. 4. Mapping AKAR on Orai1. (*A*) Ca^{2+} release and Ca^{2+} influx evoked by thapsigargin are compared between cells expressing different Orai1 N-terminal deletion constructs. (*B*) Aggregate data comparing the rate of Ca^{2+} entry are shown from experiments as in *A*. Each bar denotes data from 50 to 60 cells. (*C*) Images show NFAT1-mCherry translocation at rest and then after stimulation in cells expressing the Orai1-YFP constructs indicated. S1 denotes STIM1 and O1 Orai1. (*D*) Aggregate data from experiments as in *C* are compared. The second bar above Δ39-59 denotes the response in these cells when ionomycin was subsequently applied. Each bar is the mean of between nine and 11 cells. The symbol ** denotes comparison between control and Δ(39-59)-Orai1 in the absence of ionomycin. (*E*) Following immunoprecipitation of the indicated Orai1-YFP protein with anti-GFP antibody, samples were blotted for endogenous AKAP79. Cells were challenged with thapsigargin prior to pulldown. (*F*) NFAT1-mCherry translocation is shown following stimulation with thapsigargin and then ionomycin in cells expressing YFP-tagged Orai paralogues. (*G*) Aggregate data from several experiments as in *F* are compared. Open bars in Orai2 (O2) and Orai3 (O3) groups denote subsequent response to ionomycin. In all experiments shown, endogenous Orai1 was knocked down and untagged STIM1 (S1) was coexpressed with one of the various Orai1 constructs or paralogues. Rest denotes nonstimulated cells, and O1 KD is the response to thapsigargin in cells in which Orai1 had been knocked down. Asterisks denote comparison between O1S1 and other groups, indicated by filled bars. (*H*) Cytosolic Ca^{2+} signals over 40 min are compared for the conditions shown. These experiments were done in TKO HEK293 cells. Thapsigargin was applied at 2 μM. (*I*) Aggregate data compare NFAT1-cherry translocation for the various conditions shown, as in *H*. (*J*) Images show NFAT1-cherry translocation in cells expressing Orai1-YFP or N3-Orai1-YFP (both with STIM1) in HEK293 cells in which Orai1 had been knocked down. The right-hand panel compares aggregate data from experiments as in the left-hand panel. In *B*, *D*, *G*, *I*, and *J*, data are shown as mean± SEM. $^{**}P < 0.01$.

terminus had been spliced out and replaced with the N terminus of Orai3. As the N terminus of Orai3 lacks the AKAR domain, a prediction would be that N3-O1 should not activate NFAT. This was indeed the case (Fig. 4*J*). Robust NFAT1 movement was seen in the presence of Orai1-YFP but this was considerably less following expression of the N3-O1-YFP construct. Expression of N3-Orai1 protein resulted in a cytosolic Ca^{2+} signal that was similar to that evoked by overexpression of Orai1 (*SI Appendix*, Fig. S4). In a previous study, we had difficulty expressing the N3-Orai1 construct (synthesized by Mutagenex), gauged by the absence of a consistent Ca^{2+} signal (7). The construct we used in the present study expressed well. We do not know why the previous construct we used was much less effective.

A Peptide Mimicking AKAR Suppresses NFAT1 Activation by Leukotriene Receptors. If the stretch of amino acids we ascribe to AKAR is correct, then one would expect a peptide with the same amino acid sequence to compete with AKAR on Orai1 for binding to AKAP79. We tested this by expressing a peptide with the same sequence as AKAR (referred to as AKAR DNA). Although the peptide did not affect store-operated Ca^{2+} entry to thapsigargin (Fig. 5 *A* and *B*), it substantially reduced NFAT1-GFP migration into the nucleus (Fig. 5 *C* and *D*). Pulldown of Orai1-YFP revealed the presence of AKAP79 in thapsigargin-treated cells, but no AKAP79 was detectable in cells also expressing the peptide (Fig. 5*E*; aggregate data in Fig. 5*F*). To test this further, we used a synthetic peptide mimicking AKAR [referred to as AKAR peptide, and mimicking Orai1 (39–59)] and included it in the pull-down samples of Orai1-YFP. With the recombinant peptide present no AKAP79 was detected (Fig. 5 *E* and *F*). These data therefore demonstrate that a peptide mimicking AKAR can compete with Orai1 for AKAP79 and thereby impair NFAT1 activation.

We expressed the peptide in intact cells to test whether interaction between endogenous levels of Orai1 and AKAP79 was

essential for NFAT1 activation following stimulation of cysteinyl leukotriene receptors. Stimulation with LTC_4 evoked numerous cytosolic Ca^{2+} oscillations in both wild-type cells (Fig. 5*G*) and in cells expressing the peptide (Fig. 5*H*). Neither the number of Ca^{2+} oscillations nor the amplitude of each oscillation was affected by the presence of the peptide (Fig. 5 *I* and *J*). However, NFAT1-GFP translocation to the nucleus following stimulation with LTC_4 was almost fully suppressed by the peptide (Fig. 5 *K* and *L*). Therefore, coupling of Orai1 to AKAP79 is essential for NFAT1 translocation in response to physiological stimuli.

We carried out control experiments to rule out nonspecific effects of the AKAR peptide. First, NFAT1 nuclear translocation in peptide-expressing cells challenged with thapsigargin could be rescued by ionomycin (Fig. 5*D*, open bar). Second, scrambled AKAR peptide failed to interfere with Orai1-AKAP79 interaction in pull-down experiments (*SI Appendix*, Fig. S8). A third control, involving mutations within the AKAR peptide, is described below.

NMR Structure of the AKAR Region. Although the crystal structure of *Drosophila* Orai has been reported at 3.35-Å resolution, the construct used lacked amino acids 1 to 131. The structure therefore did not contain the N terminus of the channel, in which the AKAR region is embedded. To obtain insight into the structure of this region, we used NMR spectroscopy of the AKAR peptide.

The ensemble of calculated structures is shown in Fig. 6 in ribbon format. The peptide appears to be largely unstructured in solution. This ensemble has a relatively large rmsd of 4.65 ± 1.23 Å to the mean structure across the backbone. Although residues D16 to G19 (sequence DWIG) toward the C terminus of the peptide have backbone chemical shifts consistent with alpha-helical character, no nuclear Overhauser effects (NOEs) characteristic of secondary structure were observed, possibly due to high structural mobility of the peptide. A relatively small number of NOEs were observed for the proline-rich amino-terminal region (residues 1 to 9 in the peptide). This is consistent with the higher local rmsd average values in this region of the structure. The penta-proline section (residues 5 to 9 in the peptide) forms a loop, allowing the N and C termini to fold back on one another. This turn forms the base of a small pocket, flanked on one side by a stretch of hydrophobic amino acids interrupted by a charged

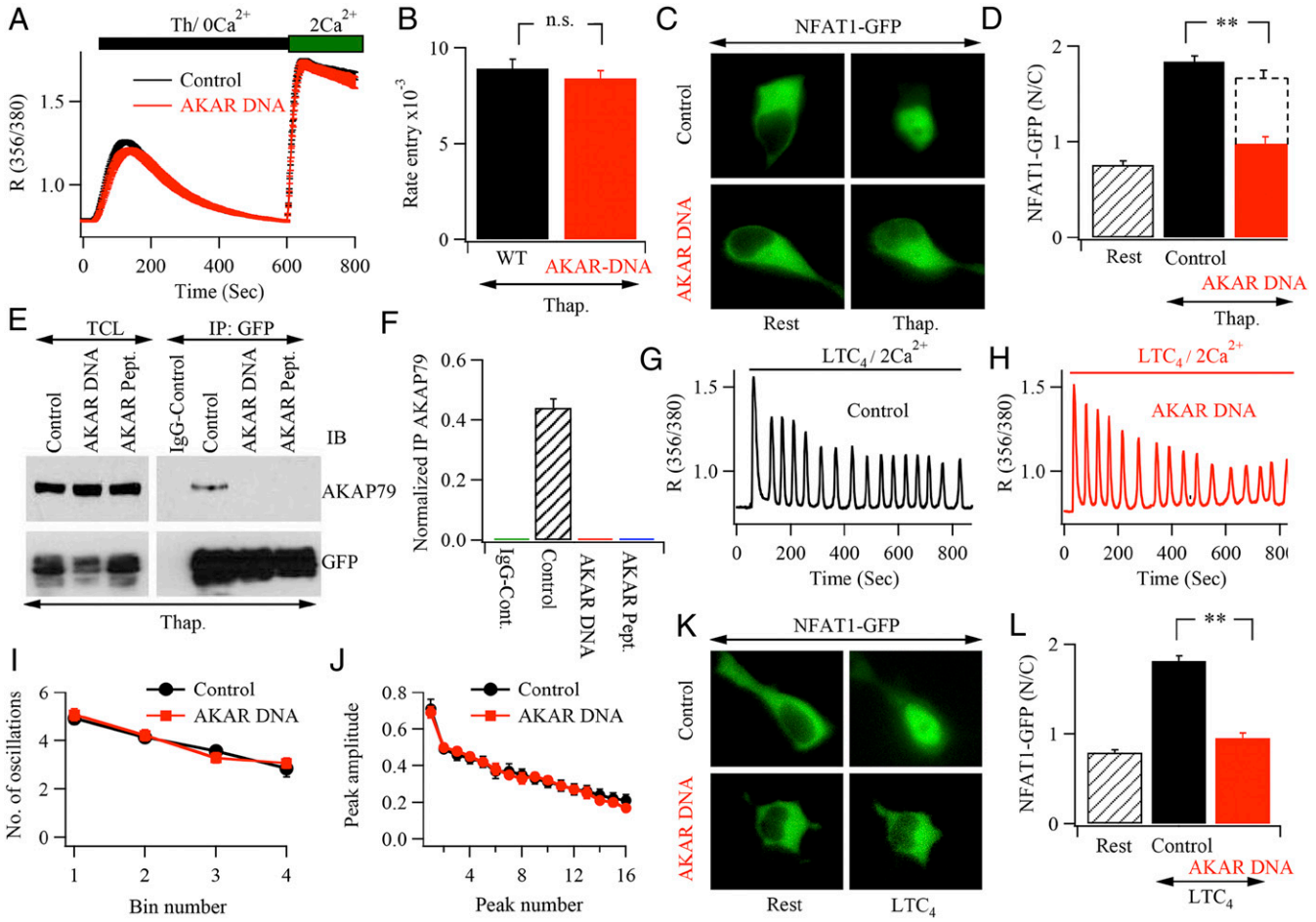

Fig. 5. A peptide mimicking AKAR inhibits NFAT1 translocation following receptor stimulation. (*A*) Store-operated Ca^{2+} entry is unaffected by expression of the peptide. (*B*) Aggregate data from experiments as in *A* are compared. (*C*) NFAT1-GFP nuclear migration is compared between a control cell and one expressing the peptide. (*D*) Aggregate data from several experiments as in *C* are compared. Open bar above AKAR DNA denotes subsequent NFAT translocation after exposure to ionomycin. Asterisks denote comparison between control and AKAR groups; the latter response was taken in the absence of ionomcyin. (*E*) Blot compares presence of endogenous AKAP79 following immunoprecipitation of Orai1-GFP. Control denotes control cells, AKAR DNA denotes cells expressing the peptide that mimicks AKAR and AKAR Pept. denotes experiments where recombinant peptide mimicking AKAR was added to the pulled-down samples. All groups were transfected with Orai1-GFP and untagged STIM1. (*F*) Aggregate data from two independent experiments as in *E* are compared. (*G*) LTC_4 evokes cytosolic Ca^{2+} oscillations in a control cell. (*H*) Ca^{2+} oscillations to LTC_4 are shown in a cell expressing peptide. (*I*) The number of Ca^{2+} oscillations in 200-s bins are compared between control cells and cells expressing peptide. (*J*) As in *I* but the amplitude of each oscillation is compared. (*K*) NFAT1-GFP translocation in response to LTC_4 challenge is compared between a control cell and one expressing peptide. (*L*) Aggregate data from experiments as in *K* are compared. In *B*, *D*, *F*, *I*, *J*, and *L*, data are shown as mean ± SEM. $^{**}P < 0.01$; n.s., not significant.

aspartate and a polar threonine residue. This pocket might favor an electrostatic interaction with a binding partner stabilized by hydrophobic interactions. To test this, we mutated all five prolines in the penta-proline loop to alanines. Unlike wild-type peptide, the mutated AKAR peptide no longer interfered with Orai1-AKAP79 interaction after store depletion (*SI Appendix*, Fig. S8), suggesting the penta-proline loop was important for function. An electrostatic surface potential map is shown in Fig. 6*C*.

Targeting AKAR Selectively Inhibits Cytokine Production, Leaving Other Orai1-Dependent Functions Intact. In RBL mast cells, activation of CRAC channels stimulates production of the cytokine interleukin 5 (IL-5) through the NFAT pathway (6). Stimulation with thapsigargin or LTC_4 led to a significant increase in IL-5 expression, and this was suppressed by either the calcineurin inhibitor cyclosporin A or after expression of AKAR peptide (Fig. 6*D*; aggregate data shown in Fig. 6*E*). Expression of AKAR peptide failed to alter the pattern of cytosolic Ca^{2+} oscillations evoked by LTC_4 (Fig. 5 *G*–*J*). Because Ca^{2+} oscillations require store refilling, which is accomplished by Ca^{2+} entry through Orai1 channels, AKAR peptide selectively uncouples Orai1 from NFAT, leaving Orai1-dependent store refilling intact. To test whether other Orai1-driven responses were also independent of Orai1-AKAP79 interaction, we examined the effects of AKAR expression on Ca^{2+}-dependent exocytosis of β-hexosaminidase. Stimulation with thapsigagin led to a large increase in secretion, and this was unaffected by the presence of AKAR peptide (Fig. 6*F*). However, secretion was blocked by the CRAC channel blocker Synta66 (Fig. 6*F*). Targeting the AKAR region therefore selectively uncouples Orai1 from the NFAT pathway.

Orai1–NFAT Coupling in MCF-7 Breast Cancer Cells. It has been suggested that store-operated Ca^{2+} entry in MCF-7 breast cancer cells is mediated exclusively by Orai3 channels (22). Knockdown of Orai3 was reported to abolish thapsigargin-evoked Ca^{2+} entry and reduce NFAT transcriptional activity by ∼30% (23). Because Orai1 is abundantly expressed in MCF7 cells (22), and Orai3 failed to activate NFAT1 in HEK293 cells (Fig. 4 *F*–*I*), we assessed whether Orai1 was able to couple to NFAT in MCF-7 cells. Stimulation with thapsigargin in Ca^{2+}-free solution led to a transient rise in cytosolic Ca^{2+} as Ca^{2+} was released from the stores (Fig. 7*A*). Readmission of 2 mM Ca^{2+} led to a small increase in cytosolic Ca^{2+}. To enhance the size of store-operated Ca^{2+}, we raised external Ca^{2+} (Fig. 7*A*), as adopted by others working with this cell type (24). Knockdown of Orai1 substantially reduced protein expression (*SI Appendix*, Fig. S10) and store-operated Ca^{2+} entry (Fig. 7*A*), as did the selective CRAC channel inhibitor Synta66 (Fig. 7*D* and ref. 25). Thapsigargin stimulation led to a significant increase in NFAT1 accumulation within the nucleus, and this was suppressed by either knockdown of Orai1 or after exposure to Synta66 (Fig. 7 *B* and *C*). A hallmark of Orai3 channels is that they are directly opened by the small molecule 2-APB, which dilates the channel pore (26–28). To see if Orai3 channels were functional in MCF-7 cells, we depleted stores with thapsigargin in Ca^{2+}-free solution and then readmitted external Ca^{2+} to allow Ca^{2+} entry through store-operated Ca^{2+} channels. Subsequent application of 2-APB led to a large subsequent rise in cytosolic Ca^{2+}(Fig. 7*D*). Pretreatment with Synta66 suppressed store-operated Ca^{2+} entry but had no effect on the subsequent response to 2-APB (Fig. 7*D*). These experiments show that 2-APB–mediated potentiation, likely via Orai3, is unaffected by Synta66, which could be explained by an earlier study that found Orai3 to be insensitive to Synta66 (29). Moreover, because Synta66 abolished store-operated Ca^{2+} entry (Fig. 7*D*), Orai1 is required for this form of Ca^{2+} influx. In cells stimulated with thapsigargin in the presence of Synta66, application of 2-APB failed to stimulate NFAT activity (Fig. 7*E*). Consistent with a major role for Orai1 (Fig. 7*C*), expression of the

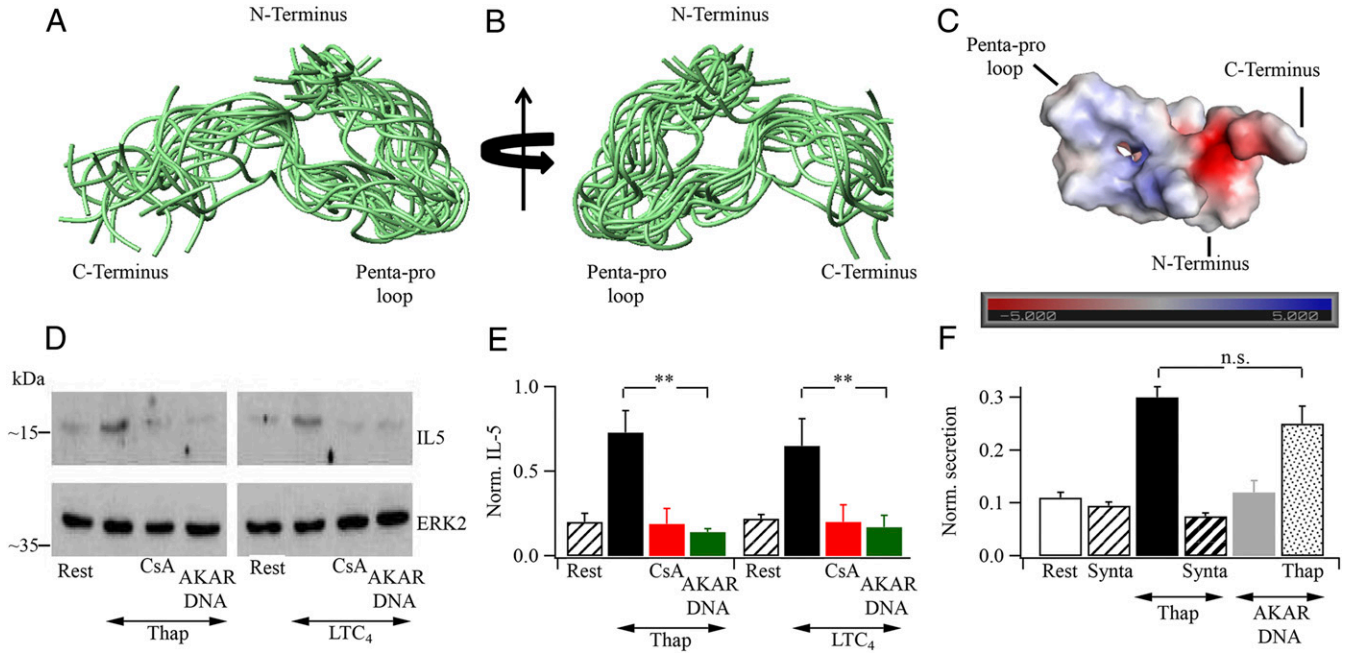

Fig. 6. NMR structure of the AKAR region. (*A*) An ensemble of 20 overlaid structures is shown. (*B*) As in *A* but the structures have been rotated 180° anticlockwise about the y axis. (*C*) Electrostatic surface potential is calculated for the structure with the lowest rms displacement from the mean. Units are k_BT/e, where k_B is the Boltzmann constant, T is the absolute temperature, and e is the magnitude of electron charge. (*D*) Western blot compares IL-5 protein expression for the conditions shown. Rest is nonstimulated cells, and CsA denotes pretreatment with 100 nM cyclosporin A for 20 min. AKAR DNA refers to transfection with AKAR plasmid 24 h prior to stimulation. (*E*) Aggregate data from two independent experiments are compared. (*F*) Bar chart compares β-hexosaminidase secretion for the conditions shown. Data are from two independent experiments. Data in *D*–*F* are from RBL cells. $^{**}P < 0.01$; n.s., not significant.

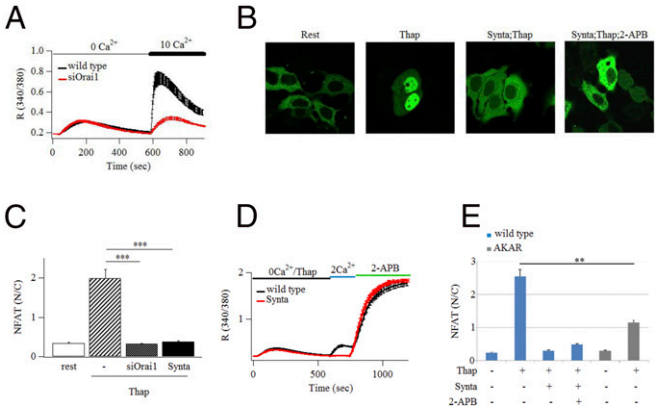

Fig. 7. Orai1 couples to NFAT in MCF-7 cells. (*A*) Store-operated Ca^{2+} entry induced by thapsigargin is significantly reduced following knockdown of Orai1. Traces are the means of between 57 and 64 cells. (*B*) Images show NFAT1-GFP nuclear distribution for the different conditions. (*C*) Aggregate data from experiments as in *B* are compared. Each bar is the mean of >37 cells. (*D*) 2-APB (50 μM) activates Ca^{2+} entry in the presence of Synta66. (*E*) Bar chart compares nuclear/cytosolic distribution of NFAT for the various conditions indicated. In *A* and *C–E*, data are shown as mean ± SEM.

AKAR plasmid significantly reduced NFAT1 activation following stimulation of CRAC channels (Fig. 7*E*).

Discussion

Ca^{2+} nanodomains that extend just a few nanometers from the Orai1 channel are necessary and sufficient to activate NFAT following physiological levels of stimulation (5, 13). Orai1 has private access to NFAT because it participates in the reversible formation of a signaling complex with AKAP79 (7). This membrane-delimited complex places calcineurin and NFAT, which are both bound to AKAP79, directly into the jurisdiction of the Ca^{2+} nanodomain arising from open Orai1 channels. This privileged line of communication between Orai1 and calcineurin enables selective activation of NFAT.

Our experiments with Orai1α and Orai1β along with Orai paralogues identify a major role for the N terminus in Orai1 in coupling to AKAP79. Consistent with this, expression of a chimeric channel containing Orai1 but with the N terminus of Orai3 failed to activate NFAT. The converse construct, Orai3 with the N terminus of Orai1, does activate NFAT (7). Deletion studies narrowed the AKAR locus to between amino acids 39 and 59. Although our coimmunoprecipitation data show an interaction between this region of Orai1 and AKAP79, it is not clear whether the two proteins bind directly or whether a bridging protein is involved. Regardless, our proximity ligation assay data show that AKAP79 and Orai1 realign to within 50 nm of one another after stimulation, the typical distance for ligation assay-dependent signals. Although AKAR comprises necessary sequences for interaction with AKAP79, it might not define the entire domain. N-terminal sequences closer to TM1 of the Orai1 channel could contribute. However, mutations close to TM1 affect conductivity and CDI of the channel because the Orai1 pore extends into the cytosol (30). Therefore, mutations beyond AKAR might have effects in addition to a possible disruption with AKAP79 binding.

Neither AKAP79 nor Orai1 directly senses the Ca^{2+} content of the store. How do the two proteins interact after store depletion? AKAP79 has been reported to associate constitutively with the pool of STIM1 in the plasma membrane (31). A recent study proposes that STIM2 couples AKAP79 to Orai1 after stimulation (32). However, knockdown of STIM2 had no inhibitory effect on activation of NFAT by agonist or thapsigargin (12), although a small amount of vestigial STIM2 might have been sufficient for coupling to take place. An alternative possibility is that STIM1 binding to Orai1 exposes the AKAR domain, increasing the probability that AKAP79 associates with the channel.

Within the AKAR region of Orai1 is an inverted caveolin-binding consensus site (33) containing three aromatic amino acids (Y52, W55, and Y60). However, in the cell types we have used we have failed to detect caveolin-1 protein expression (34). Moreover, mutation of both Y52 and W55 to alanines in Orai failed to interfere with NFAT-dependent gene expression, suggesting little role for caveolin.

It is generally assumed that tethered enzymes like calcineurin, once released from the constraints of a scaffolding protein, activate cytosolic substrates such as NFAT. Our experiments comparing AKAP79 with the mutant protein AKAP79ΔLZ that is unable to bind NFAT show that only NFAT attached to AKAP79 can be activated by Ca^{2+} nanodomains from Orai1. Our findings are consistent with a recent study that showed coupling of Cav1.2 channels to NFAT required the transcription factor to be tethered to AKAP79 (16). The insensitivity of the cytosolic pool to activated calcineurin is not because calcineurin remains tethered to AKAP79. Ca^{2+} entry through CRAC channels releases calcineurin from AKAP79 (5) and the enzyme subsequently migrates into the nucleus (5, 35). Why is the pool of NFAT tethered to AKAP79 and activated by CRAC channels sufficient for gene transcription without needing an additional contribution from cytosolic NFAT1? First, we have shown that NFAT1 accumulates in the nucleus with a half-time of ~8 min following opening of CRAC channels (13), whereas rephosphorylation by cytosolic protein kinases has a half-time of >20 min and nuclear rephosphorylation is even slower (6). Pulses of Ca^{2+} through CRAC channels that last just a few minutes are therefore sufficient to activate NFAT significantly. Second, calcineurin has been found to migrate into the nucleus following stimulation in a complex with NFAT (36), thereby ensuring the transcription factor remains dephosphorylated as it runs the gauntlet of cytosolic and nuclear protein kinases. If NFAT1 remains associated with calcineurin, then cytosolic phosphorylated NFAT would have restricted access to the phosphatase. Finally, phosphorylated NFAT is not free in the cytosol but accumulates in a complex that contains those protein

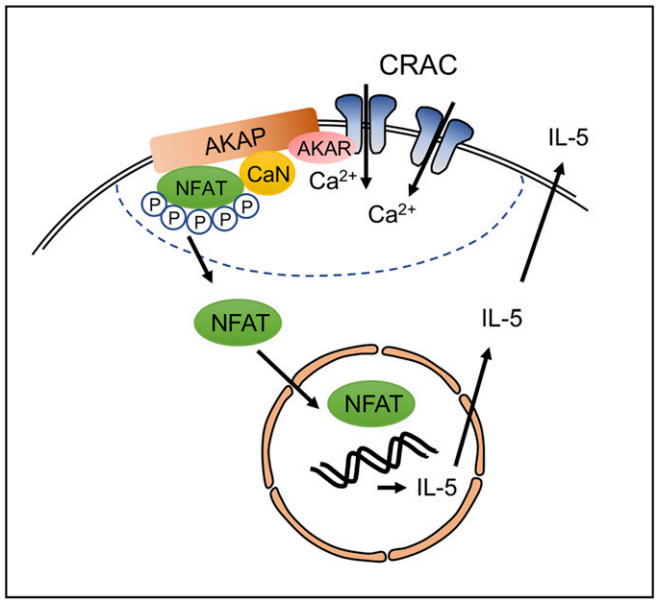

Fig. 8. Cartoon summary of our key findings. A membrane-delimited signalosome forms between AKAR on the N terminus of Orai1 and AKAP79, which accommodates calcineurin and inactive (phosphorylated) NFAT1. For simplicity, AKAP79 is shown as directing interacting with AKAR, but the interaction could be mediated through a bridging protein.

kinases that phosphorylate and inhibit NFAT but in which calcineurin is absent (37). Limited accessibility of calcineurin, released from AKAP79, to this pool of NFAT might occur. These findings should not be taken to suggest that cytosolic NFAT cannot be activated by cytosolic calcineurin. We previously showed that a non-physiologically large and sustained bulk cytosolic Ca^{2+} rise, evoked by stimulation with thapsigargin when Ca^{2+} extrusion is blocked (38), or after exposure to a high concentration of ionomycin (e.g., Figs. 1*K* and 4*D*), can partially activate NFAT1. However, cytosolic Ca^{2+} does not reach these levels physiologically.

Our findings add a further dimension to the concept of local signaling. The entire Ca^{2+} nanodomain/AKAP79/calcineurin/NFAT pathway activates close to Orai1 channels, ensuring NFAT activation reflects Orai1 activity (Fig. 8). This secures a private line of communication between CRAC channels and gene transcription. Consistent with selective activation of tethered NFAT, recruitment of only ~30% of the total NFAT pool is sufficient for robust NFAT1-dependent gene transcription following CRAC channel stimulation (39).

In polarized pancreatic acinar cells and *Xenopus* oocytes it has been found that local Ca^{2+} entry through CRAC channels is first taken up by peripheral endoplasmic reticulum and then the Ca^{2+} tunnels through the organelle lumen before being released by $InsP_3$ receptors to reach target sites located away from the CRAC channels (40). Our findings that knockdown of AKAP79 or expression of AKAR peptide both inhibited NFAT1 translocation without affecting $InsP_3$-driven cytosolic Ca^{2+} oscillations demonstrate that it is local Ca^{2+} entry itself and not Ca^{2+} uptake followed by $InsP_3$-dependent Ca^{2+} release that is important for activating NFAT1. However, we have shown that accumulation of NFAT4 in the nucleus requires both local Ca^{2+} entry through CRAC channels and a rise in nuclear Ca^{2+} (6), the latter being accomplished by Ca^{2+} entry through CRAC channels tunneling through the endoplasmic reticulum to reach the nuclear envelope. The combination of direct activation of targets by Ca^{2+} nanodomains near CRAC channels in conjunction with Ca^{2+} tunneling will increase the breadth of processes that can be regulated by local Ca^{2+} signaling.

Following its introduction in the 1980s, the calcineurin inhibitor cyclosporin A has transformed organ transplantation by greatly diminishing acute rejection rates. Tacrolimus, another calcineurin blocker, is even more effective in reducing organ rejection. However, patients on either drug have elevated blood pressure and suffer from serious chronic nephrotoxicity issues (41, 42). Block of Orai1 prevents calcineurin activation in immune cells but has the downside of interfering with all other Orai1-dependent functions including refilling of Ca^{2+} stores and mitochondrial energy production and secretion. Our identification of the AKAR site on Orai1 and our demonstration that targeting AKAR suppresses the NFAT pathway leaving other Orai1-dependent functions including secretion and store refilling intact opens up the possibility for engineered therapies that target only certain consequences of Orai1 activation. Importantly, unlike the case with channel pore blockers, targeting AKAR would not only retain other Orai1-dependent functions but would have no impact on Orai2, Orai3, or even short Orai1. The NMR structure of AKAR we report reveals a penta-proline loop that forms the base of a small pocket flanked by a stretch of hydrophobic amino acids. Mutation of these prolines to alanines prevented the peptide from suppressing Orai1–AKAP79 interaction, suggesting the proline-driven structural twist is important for function. Targeting the pocket with small-molecule inhibitors to disengage the AKAP79–Orai1 interaction could potentially lead to a new family of targeted immunosuppressants.

Materials and Methods

Details of generation of a CRISPR-Cas9 knockout HEK293 cell line lacking all three Orai1 isoforms, HEK293, RBL, and MCF-7 cell culture, siRNA-mediated knockdowns, plasmid constructs and transfections, mutagenesis, synthetic peptides, proximity ligation assay, NFAT nuclear translocation, fluorescence-activated cell sorting for NFAT-driven reporter gene expression, secretion of β-hexosaminidase, cytosolic Ca^{2+} measurements with chemical indicators, coimmunoprecipitation, Western blot analysis, NMR, and statistics are provided in *SI Appendix*.

Data Availability. All study data are included in the article and/or *SI Appendix*.

ACKNOWLEDGMENTS. This work was supported by a Medical Research Council Programme Grant to A.B.P. (Grant L01047X) and by the Intramural Research Program of the NIH, National Institute of Environmental Health Sciences. We acknowledge the Micron Advanced Bioimaging Unit (supported by Wellcome Strategic Awards 091911/B/10/Z and 107457/Z/15/Z) for their support and assistance in this work. R.B. and M.A.H. were funded by Swiss National Science Foundation Sinergia Grants CRS115_180326 and CRS113_160782.

1. A. Rao, C. Luo, P. G. Hogan, Transcription factors of the NFAT family: Regulation and function. *Annu. Rev. Immunol.* **15**, 707–747 (1997).
2. P. G. Hogan, L. Chen, J. Nardone, A. Rao, Transcriptional regulation by calcium, calcineurin, and NFAT. *Genes Dev.* **17**, 2205–2232 (2003).
3. E. M. Gallo, K. Canté-Barrett, G. R. Crabtree, Lymphocyte calcium signaling from membrane to nucleus. *Nat. Immunol.* **7**, 25–32 (2006).
4. S. Feske *et al.*, A mutation in Orai1 causes immune deficiency by abrogating CRAC channel function. *Nature* **441**, 179–185 (2006).
5. P. Kar, A. B. Parekh, Distinct spatial Ca2+ signatures selectively activate different NFAT transcription factor isoforms. *Mol. Cell* **58**, 232–243 (2015).
6. P. Kar, G. R. Mirams, H. C. Christian, A. B. Parekh, Control of NFAT isoform activation and NFAT-dependent gene expression through two coincident and spatially segregated intracellular Ca2+ signals. *Mol. Cell* **64**, 746–759 (2016).
7. P. Kar *et al.*, Dynamic assembly of a membrane signaling complex enables selective activation of NFAT by Orai1. *Curr. Biol.* **24**, 1361–1368 (2014).
8. Y. Gwack *et al.*, Biochemical and functional characterization of Orai proteins. *J. Biol. Chem.* **282**, 16232–16243 (2007).
9. M. Fukushima, T. Tomita, A. Janoshazi, J. W. Putney, Alternative translation initiation gives rise to two isoforms of Orai1 with distinct plasma membrane mobilities. *J. Cell Sci.* **125**, 4354–4361 (2012).
10. J. Di Capite, S.-W. Ng, A. B. Parekh, Decoding of cytoplasmic Ca(2+) oscillations through the spatial signature drives gene expression. *Curr. Biol.* **19**, 853–858 (2009).
11. S. W. Ng *et al.*, Cysteinyl leukotriene type I receptor desensitization sustains Ca2+-dependent gene expression. *Nature* **482**, 111–115 (2012).
12. P. Kar, D. Bakowski, J. Di Capite, C. Nelson, A. B. Parekh, Different agonists recruit different stromal interaction molecule proteins to support cytoplasmic Ca2+ oscillations and gene expression. *Proc. Natl. Acad. Sci. U.S.A.* **109**, 6969–6974 (2012).
13. P. Kar, C. Nelson, A. B. Parekh, Selective activation of the transcription factor NFAT1 by calcium microdomains near Ca2+ release-activated Ca2+ (CRAC) channels. *J. Biol. Chem.* **286**, 14795–14803 (2011).
14. X. Zhang *et al.*, A calcium/cAMP signaling loop at the ORAI1 mouth drives channel inactivation to shape NFAT induction. *Nat. Commun.* **10**, 1971 (2019).
15. H. Li *et al.*, Balanced interactions of calcineurin with AKAP79 regulate Ca2+-calcineurin-NFAT signaling. *Nat. Struct. Mol. Biol.* **19**, 337–345 (2021).
16. J. G. Murphy, K. C. Crosby, P. J. Dittmer, W. A. Sather, M. L. Dell'Acqua, AKAP79/150 recruits the transcription factor NFAT to regulate signaling to the nucleus by neuronal L-type Ca^{2+} channels. *Mol. Biol. Cell* **30**, 1743–1756 (2019).
17. M. G. Gold *et al.*, Architecture and dynamics of an A-kinase anchoring protein 79 (AKAP79) signaling complex. *Proc. Natl. Acad. Sci. U.S.A.* **108**, 6426–6431 (2011).
18. B. A. McNally, A. Somasundaram, A. Jairaman, M. Yamashita, M. Prakriya, The C- and N-terminal STIM1 binding sites on Orai1 are required for both trapping and gating CRAC channels. *J. Physiol.* **591**, 2833–2850 (2013).
19. I. Frischauf *et al.*, Cooperativeness of Orai cytosolic domains tunes subtype-specific gating. *J. Biol. Chem.* **286**, 8577–8584 (2011).
20. M. Yamashita, L. Navarro-Borelly, B. A. McNally, M. Prakriya, Orai1 mutations alter ion permeation and Ca2+-dependent fast inactivation of CRAC channels: Evidence for coupling of permeation and gating. *J. Gen. Physiol.* **130**, 525–540 (2007).
21. R. E. Yoast *et al.*, The native ORAI channel trio underlies the diversity of Ca^{2+} signaling events. *Nat. Commun.* **11**, 2444 (2020).
22. R. K. Motiani, I. F. Abdullaev, M. Trebak, A novel native store-operated calcium channel encoded by Orai3: Selective requirement of Orai3 versus Orai1 in estrogen receptor-positive versus estrogen receptor-negative breast cancer cells. *J. Biol. Chem.* **285**, 19173–19183 (2010).
23. R. K. Motiani *et al.*, Orai3 is an estrogen receptor α-regulated Ca^{2+} channel that promotes tumorigenesis. *FASEB J.* **27**, 63–75 (2013).
24. M. Faouzi *et al.*, Down-regulation of Orai3 arrests cell-cycle progression and induces apoptosis in breast cancer cells but not in normal breast epithelial cells. *J. Cell. Physiol.* **226**, 542–551 (2011).
25. S.-W. Ng, J. di Capite, K. Singaravelu, A. B. Parekh, Sustained activation of the tyrosine kinase Syk by antigen in mast cells requires local Ca2+ influx through Ca2+ release-activated Ca2+ channels. *J. Biol. Chem.* **283**, 31348–31355 (2008).
26. A. Lis *et al.*, CRACM1, CRACM2, and CRACM3 are store-operated Ca2+ channels with distinct functional properties. *Curr. Biol.* **17**, 794–800 (2007).

27. R. Schindl *et al*., 2-aminoethoxydiphenyl borate alters selectivity of Orai3 channels by increasing their pore size. *J. Biol. Chem.* **283**, 20261–20267 (2008).
28. M. Yamashita, A. Somasundaram, M. Prakriya, Competitive modulation of Ca2+ release-activated Ca2+ channel gating by STIM1 and 2-aminoethyldiphenyl borate. *J. Biol. Chem.* **286**, 9429–9442 (2011).
29. J. Li *et al*., Orai3 surface accumulation and calcium entry evoked by vascular endothelial growth factor. *Arterioscler. Thromb. Vasc. Biol.* **35**, 1987–1994 (2015).
30. F. M. Mullins, M. Yen, R. S. Lewis, Orai1 pore residues control CRAC channel inactivation independently of calmodulin. *J. Gen. Physiol.* **147**, 137–152 (2016).
31. J. L. Thompson, T. J. Shuttleworth, Anchoring protein AKAP79-mediated PKA phosphorylation of STIM1 determines selective activation of the ARC channel, a store-independent Orai channel. *J. Physiol.* **593**, 559–572 (2015).
32. G. Y. Son *et al*., STIM2 targets Orai1/STIM1 to the AKAP79 signaling complex and confers coupling of Ca^{2+} entry with NFAT1 activation. *Proc. Natl. Acad. Sci. U.S.A.* **117**, 16638–16648 (2020).
33. F. Yu, L. Sun, K. Machaca, Constitutive recycling of the store-operated Ca2+ channel Orai1 and its internalization during meiosis. *J. Cell Biol.* **191**, 523–535 (2010).
34. Y.-C. Yeh, A. B. Parekh, Distinct structural domains of caveolin-1 independently regulate Ca2+ release-activated Ca2+ channels and Ca2+ microdomain-dependent gene expression. *Mol. Cell. Biol.* **35**, 1341–1349 (2015).
35. W. I. Al-Daraji, K. R. Grant, K. Ryan, A. Saxton, N. J. Reynolds, Localization of calcineurin/NFAT in human skin and psoriasis and inhibition of calcineurin/NFAT activation in human keratinocytes by cyclosporin A. *J. Invest. Dermatol.* **118**, 779–788 (2002).
36. F. Shibasaki, E. R. Price, D. Milan, F. McKeon, Role of kinases and the phosphatase calcineurin in the nuclear shuttling of transcription factor NF-AT4. *Nature* **382**, 370–373 (1996).
37. S. Sharma *et al*., Dephosphorylation of the nuclear factor of activated T cells (NFAT) transcription factor is regulated by an RNA-protein scaffold complex. *Proc. Natl. Acad. Sci. U.S.A.* **108**, 11381–11386 (2011).
38. Y.-P. Lin, D. Bakowski, G. R. Mirams, A. B. Parekh, Selective recruitment of different Ca^{2+}-dependent transcription factors by STIM1-Orai1 channel clusters. *Nat. Commun.* **10**, 2516 (2019).
39. P. Kar, C. Nelson, A. B. Parekh, CRAC channels drive digital activation and provide analog control and synergy to Ca(2+)-dependent gene regulation. *Curr. Biol.* **22**, 242–247 (2012).
40. O. H. Petersen, R. Courjaret, K. Machaca, Ca^{2+} tunnelling through the ER lumen as a mechanism for delivering Ca^{2+} entering via store-operated Ca^{2+} channels to specific target sites. *J. Physiol.* **595**, 2999–3014 (2017).
41. A. C. Wiseman, Immunosuppressive medications. *Clin. J. Am. Soc. Nephrol.* **11**, 332–343 (2016).
42. M. Naesens, D. R. Kuypers, M. Sarwal, Calcineurin inhibitor nephrotoxicity. *Clin. J. Am. Soc. Nephrol.* **4**, 481–508 (2009).